

# Lunar liquid mirror telescope: structural concepts

Peter Klimas\*<sup>a</sup>, Neil Rowlands<sup>a</sup>, Paul Hickson<sup>b</sup>, Ermanno F. Borra<sup>c</sup>, Simon Thibault<sup>c</sup>

<sup>a</sup>COM DEV Space Systems, #100 303 Terry Fox Drive, Ottawa, ON, Canada, K2K 3J1

<sup>b</sup>Dept. of Physics & Astronomy, University of British Columbia, 6224 Agricultural Rd.,  
Vancouver, B.C., Canada, V6T 1Z1.

<sup>c</sup>Dép. de physique, de génie physique et d'optique, Pavillon d'optique-photonique,  
Université Laval, Québec, Canada, G1K 7P4

## ABSTRACT

The potential of a return of human presence to the Moon, raises the possibility of significant lunar infrastructure and with it the possibility of astronomical installations which can make use of the lunar surface as a stable platform and take advantage of the lack of atmosphere. Studies have been done in the US and Canada on the feasibility of such installations, and in particular studies of large lunar liquid mirror telescopes have been performed. We report here on the structural design concepts undertaken for one of these studies.

**Keywords:** Liquid mirror, lunar telescope, large aperture telescope, ultra-violet telescope

## 1. INTRODUCTION

Given that detector technology and optical technology can achieve near 100% efficiency for the transmission and detection of photons, the primary means of obtaining higher sensitivity astronomical observations is via larger apertures. For point source sensitivity, large apertures provide both larger collecting area and better angular resolution – assuming they are limited by diffraction. This is why the worldwide astronomical community is currently extensively studying the implementation of large (>20 m) telescopes. A key element of these proposed ground-based telescopes is adaptive optics systems which correct for the effects of atmospheric seeing (blurring) and provide improved point source sensitivity.

Since space-based telescopes do not have the atmospheric seeing constraint, their point source sensitivity is constrained only by their size and achievable optical quality. This is why the Hubble Space Telescope remains a scientifically highly productive observatory in the era of 8 m ground based telescopes. Understandably there is great interest in large space-based telescopes, even beyond the capabilities of the James Webb Space Telescope. JWST is a 6.5 m diameter telescope optimized for the near to mid-infrared (2 to 28  $\mu\text{m}$ ) wavelength. There is great scientific interest in both larger diameter space-borne telescopes and space-borne telescopes with expanded wavelength coverage [1] & [2]. Expanding to the ultraviolet and visible spectrum with a large (deployable) space-borne telescope is challenging due to the much higher surface accuracy required on the primary mirror. Concepts for 8 m to 16 m diameter space-borne ultraviolet / visible telescopes are actively being explored [3] & [4]. Another option for a large aperture space telescope is the construction of a large lunar telescope. This option is viable if there is to be a significant infrastructure available at a suitable location on the moon. One concept for such a telescope is a large aperture zenith pointing liquid mirror telescope. Such a concept was explored in a NASA NIAC study [5].

These mission concepts have the goal of achieving 5-10x the angular resolution of JWST, with a corresponding greater increase in point source sensitivity. The point source sensitivity (the reciprocal of the integration time needed to reach a given signal-to-noise ratio) for a perfect telescope is given by (where D is the diameter of the telescope and  $\lambda$  is the operating wavelength):

$$S_0 = (3\pi^2 - 16)D^4 / 48\lambda^2 \quad (1)$$

\*[peter.klimas@comdev.ca](mailto:peter.klimas@comdev.ca); phone 1 613 591-7777; fax 1 613 591-7789; [comdev.com](http://comdev.com)

Table 1 shows a comparison of equivalent ideal telescopes, based solely on equation (1), for various missions. Gemini is an 8 m ground based telescope and assuming that the adaptive optics upgrades for this observatory can achieve diffraction limited performance in the visible, then its point source sensitivity will exceed JWST. However this will be true only over small fields of view and for wavelengths less than 2.0  $\mu\text{m}$  due to the thermal background. ATLAST-16 represents the largest aperture space telescope which would be feasible with the next generation of heavy lift launchers such as the Ares-V [4]. The last column in Table 1 is the entry for a potential large lunar liquid mirror telescope (LLMT). The key assumptions in the comparison of ATLAST and LLMT is that ATLAST will have a longer diffraction limited wavelength than LLMT and that LLMT has the potential for a larger aperture than ATLAST.

**Table 1: Ideal Telescope Point Source Sensitivity Comparison**

	Hubble	JWST	Gemini AO	ATLAST-16	LLMT
Diameter (m)	2.4	6.5	8	16	20
Diffraction Limited Wavelength ( $\mu\text{m}$ )	0.3	2.0	0.5	0.5	0.3
Relative Point Source Sensitivity	0.8	1.0	37	587	3984

This first assumption is justified by the JWST experience. Despite an early desire to include capability to wavelengths as short as possible (0.6  $\mu\text{m}$  and below), the difficulties in lightweight optics manufacture and in accurate deployment and tuning of these optics on-orbit have resulted in JWST being optimized around its infrared point source sensitivity, where its key scientific objectives remain. The difficulties in obtaining short wavelength coverage with JWST highlight the potential issues for mission concepts such as ATLAST. Thus for this comparison we optimistically estimate a 4x improvement over JWST's primary mirror figure accuracy and hence diffraction limit for ATLAST.

A liquid mirror telescope provides a significant advantage over other ultraviolet / visible deployable telescope technologies since the rotating liquid will very accurately follow an equipotential surface, thus providing a highly smooth surface suitable for the shortest wavelengths. Optical quality test of large ground-based liquid mirror telescopes have demonstrated their potential for diffraction limited performance down to the blue and even UV wavelength range [6]. The key requirement for a liquid mirror is a means to rotate the system and a force of constant acceleration. While a constant force of acceleration is easily obtained on the surface of any of the solar system's larger solid bodies, the disadvantage is that the telescope must point in the direction of the constant acceleration. On a solid body this limits the observable field of view to very near local zenith. Fortunately at the largest scales, the universe is extremely isotropic, and there is no preferred direction to examine the early universe. Since the integration times to achieve the required point source sensitivities are very long, a zenith pointing telescope will achieve most of the cosmological science objectives of an equivalent steerable telescope. For a zenith pointing telescope on a rotating body, the rotation and precession can provide a slow scan of moderate large field of view.

From Table 1, it can be seen that a large lunar liquid mirror telescope (LLMT) with ultraviolet imaging capability has the potential for three orders of magnitude sensitivity increase over JWST and Hubble and an order of magnitude sensitivity greater than even the forward looking plans for large space-borne telescopes. The other key assumption in this comparison is the potential mass (and hence cost) savings of an LLMT, when compared to current large space-borne deployable telescope technology, ie JWST. A metric for comparing primary mirror technology is the ratio of primary mirror mass to primary mirror area. When the technology development for JWST started a decade ago, a goal of 10  $\text{kg}/\text{m}^2$  was set for the JWST primary mirror – this includes all the systems needed to achieve the surface figure, so in this case also includes the primary mirror actuators that are used to “tune” the figure of the mirror. Although not quite achieving its goal JWST achieved 15  $\text{kg}/\text{m}^2$ , still significantly better than the monolithic technology of HST at 50  $\text{kg}/\text{m}^2$ . Estimating the achievable mass per area for a plausible LLMT support structure is the topic of this paper.

## 2. STRUCTURAL DESIGN OF LARGE LUNAR LIQUID MIRROR TELESCOPES

### 2.1. Design Considerations

The structural design of the Lunar Liquid Mirror Telescope (LLMT) is driven by the optical requirements of a 20 m diameter parabolic surface that can reach an optical grade surface when 1 mm of liquid is uniformly distributed through centrifugal forces. Furthermore, as the telescope's anticipated deployment is on the lunar surface, mass and assembly considerations are of great importance.

Potential conceptual optical designs of a wide field (15°x15°) LLMT have been developed. These on-axis three mirror designs are shown in Figure 2-1 & Figure 2-2. Driven by the optical design considerations, it has been concluded that two possible positions for the fold mirror are possible, above or below the primary mirror (referred to as case 1 and 2). These two options are represented in the optical raytrace diagrams below.

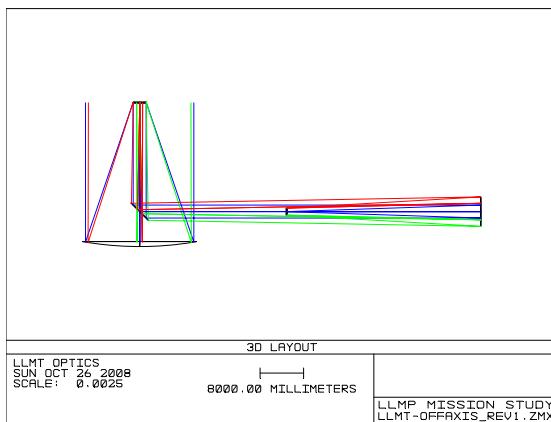


Figure 2-1: Case 1 optical design

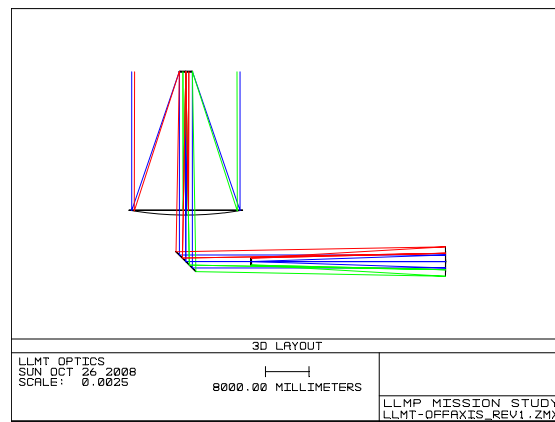


Figure 2-2: Case 2 optical design

The fold mirror location has direct impact on structural design and bearing selection. Implementing a more conventional design with the fold mirror below the primary mirror allows supporting the fold mirror and other “down-light” components at ground level, alleviating their support structure requirements. Unfortunately, this has the drawback of increasing bearing mass by forcing the use of a large ring bearing (through which the fold mirror can be supported) and increasing the mass of the primary mirror support structure as the primary mirror and bearing will have to be supported above the fold mirror to keep the light-path unobstructed. Furthermore, an approximate 6 m increase in the height of the LLMT will intensify assembly complexity.

In contrast, allowing the fold to be above the primary mirror allows for flexibility in the bearing design (possible to support the fold mirror from below or suspend from above) while also lowering the primary mirror structure. This translates to a reduced bearing mass and primary mirror support structure while increasing the mass of the fold mirror and “down-light” component support structure.

### 2.2. Design Selection

With these design considerations in mind, it was decided that the LLMT should have a light-weight primary mirror surface supported by ribs which distribute the load onto a truss system attached to the bearing. Depending on the selected design, the bearing would then be fixed to a supporting structure elevating the primary mirror structure above the fold mirror, or directly fixed to the ground.

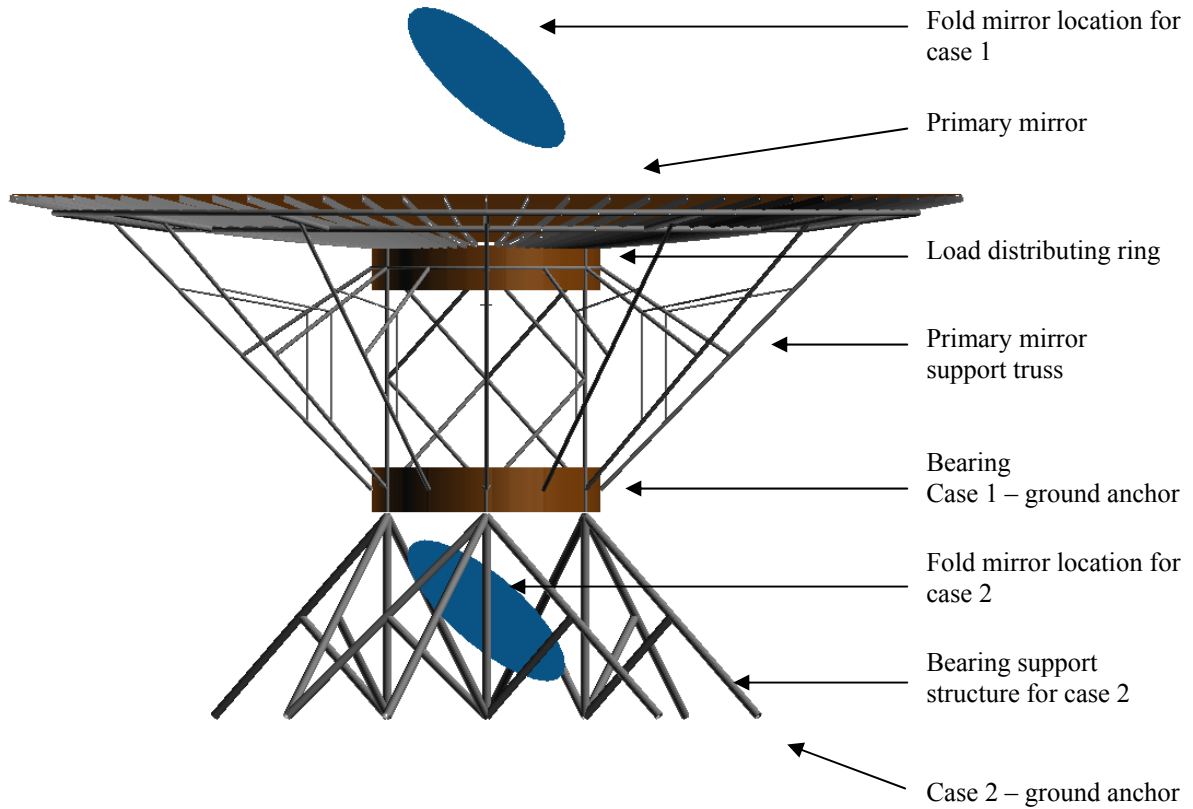


**Figure 2-3: Structural concept of a large lunar liquid mirror telescope**

### 2.3. Primary Mirror Structure

As the primary mirror must disassemble into sections for transport, a stiff (stackable for transport) panel design is preferred. As it would be very difficult to make the seams of the individual panels impregnable to the liquid, a thin membrane would be required to be rolled out on the assembled mirror surface. Furthermore, these panels would need to be light-weight and must support the reflective liquid without sag between truss elements. Since primary mirror stiffness is paramount, the supporting rib structure must have this characteristic. As loading on rib members will only include a combination of gravity and centrifugal forces, sections with non-symmetric stiffness characteristic are well suited allowing for weight reduction. In general, square sections are stiffer than round sections of an equivalent diameter, while rectangular sections with the long axis oriented in the plane of the load are even stiffer. An I-section will have comparable stiffness to an equivalently sized rectangular section with the advantage of mass savings. Due to transportation and assembly considerations, a rectangular section was selected for the design study. Using a rectangular section, one can take advantage of the ability to telescope sections or simply sliding (radially) sections onto each other and pinning to constrain movement in all six degrees of freedom.



**Figure 2-4: Rib sections supporting mirror surface panels**

## 2.4. Truss Design

The mirror truss system must support the primary mirror panels and ribs anchoring them to the bearing structure. Therefore, the truss must have the ability to carry loads in all directions during acceleration, deceleration and other dynamic perturbations. Circular tubing is ideal for these conditions and therefore was selected.

## 2.5. Bearing Design

Due to low bearing vibration requirements, two distinct types of bearings are feasible for LLMT, electromagnetic and fluid bearings. The selection between an electromagnetic or fluid bearing is considered out of the scope of this document.

Structurally, both these bearing types can be designed as large ring bearings or smaller solid bearings. The advantage of large ring bearings includes high tilt stiffness and the ability to construct a support structure through the bearing hole (simpler to implement the fold mirror support), but will require a support structure to keep it true. A solid bearing, in comparison, has a lower mass and requires a less rigid support structure, but is less stiff and requires the fold mirror to be suspended from the secondary mirror structure.

Lastly, to keep the bearing aligned and dust free, the bearing and its support structure would have to be launched as a single sealed unit, therefore favoring a solid bearing from a transportation consideration.

Listed Table 2 are the bearing mass assumptions for 5 m diameter ring bearings constructed of various materials, along with estimates for a 1 m solid bearing and a 0.75 m superconducting bearing. The bearing used for this design study has an approximated tilt stiffness of  $1.7 * 10^9$  N-m/rad and was approximated through extrapolation from currently available commercial products.

**Table 2 Bearing Mass Assumptions**

Type	Material	Mass
Ring – 5 m aperture	Ti Alloy 6Al-4V	1375 kg
	Al Alloy 7075-T751	866 kg
	Al Alloy 2090-T83	800 kg
	Mg Alloy AZ91	560 kg
Solid – 1 m diameter	Ti Alloy 6Al-4V	275 kg
Superconducting - 0.75 m diameter	various	300 kg

## 2.6. Structural Analysis

A NASTRAN finite element model was built to test the properties of the two selected design cases by varying the bearing support structure.

After initial experimentation, it was quickly determined that high-stiffness and lightweight composite materials must be used to be within reach of the mass budget of  $5 \text{ kg/m}^2$ . Furthermore, it was determined that the surface panels of the primary mirror must be composed of a stiff honeycomb composite to avoid undesirable sag. The mirror surface was modeled as a PSHELL element mimicking honeycomb properties while the remainder of the structure was modeled using beam elements of various cross-sections. The bearing was modeled as six springs (one for each degree of freedom) with an estimated tilt stiffness of  $1.7 * 10^9$  N-m/rad. The primary mirror and supporting structure mass for case 1 and case 2 are estimated at approximately 2000 kg and 2650 kg respectively.

## 2.7. Static analysis for lunar gravity loading

A static analysis was performed using lunar gravity loading of  $1.622 \text{ m/s}^2$ . The liquid mass of 400 kg was approximated by a pressure load of 650 N distributed over the mirror surface. The calculated mirror sag from gravity is in the order of 2 mm and therefore must be considered during parabolic curvature design.

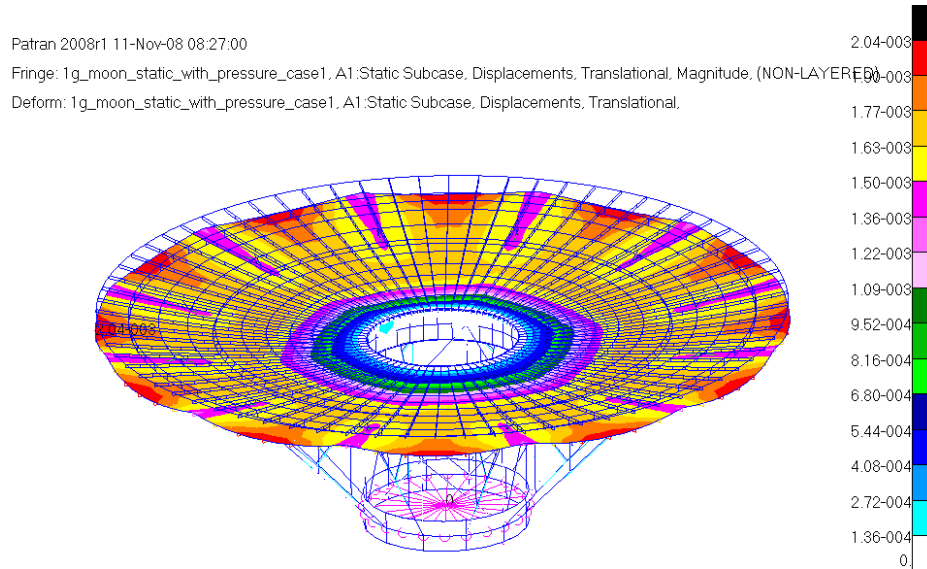


**Figure 2-5: Lunar gravity loading - case 1**

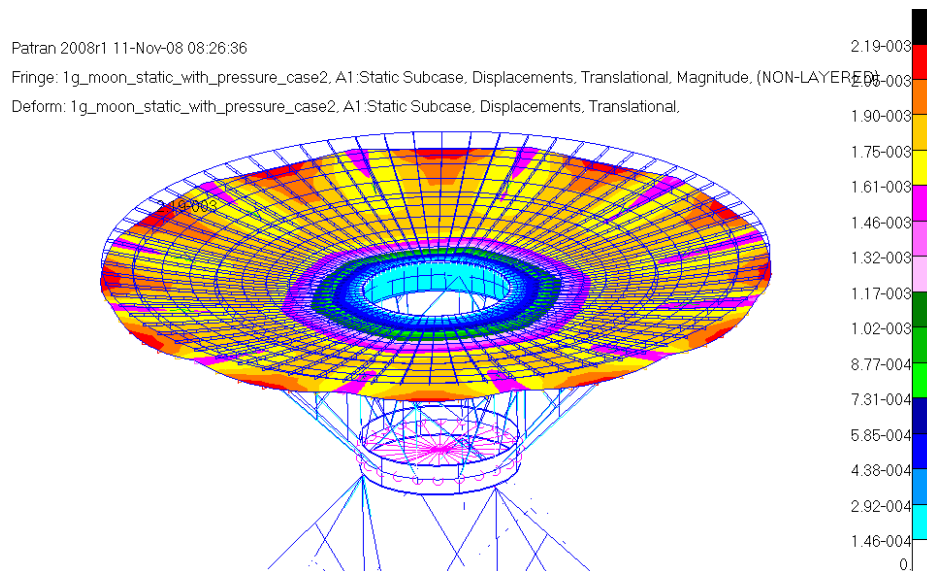


**Figure 2-6: Lunar gravity loading - case 2**

## 2.8. Combined lunar gravity and rotational loading

As seen in the figures below, the addition of rotational loading caused by the mirror rotation of 9.4 %/s results in a marginal increase (below 1%) in the deflection of the mirror surface.

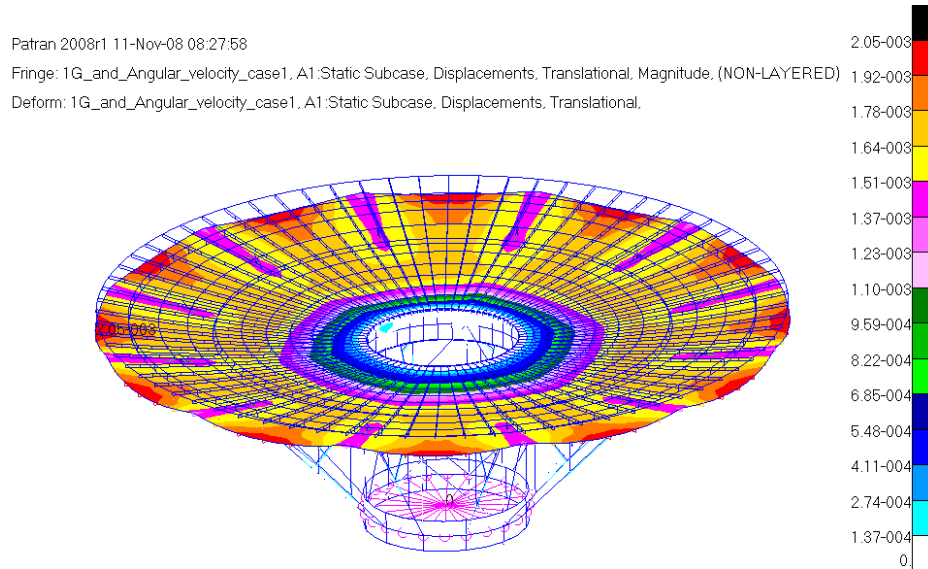


**Figure 2-7: Centripetal and lunar gravity loading – case 1**

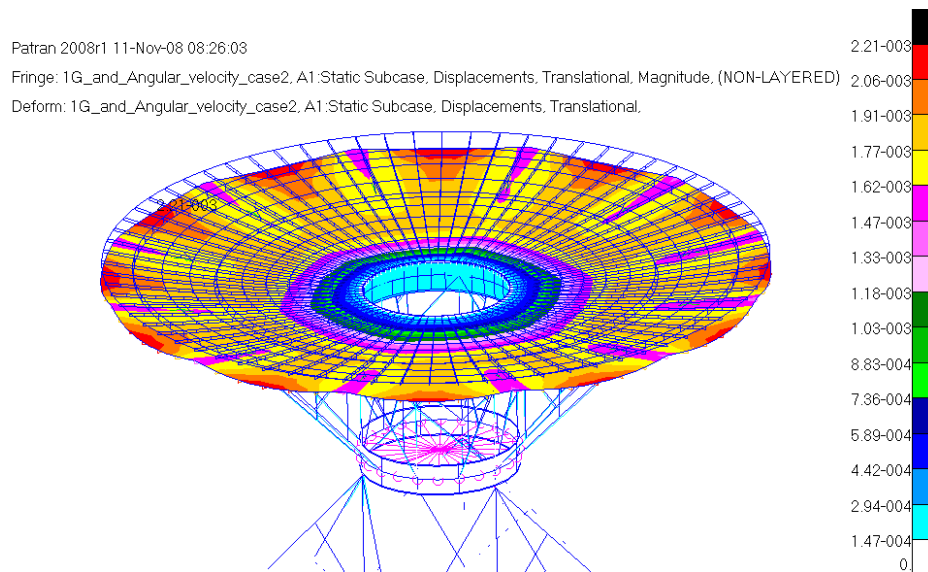


**Figure 2-8: Centripetal and lunar gravity loading – case 2**

## 2.9. Stiffness characterization

The stiffness characterization of the mirror structure was determined by applying a moment (through two opposing loads) on the mirror structure and measuring the deflection. This is a similar method to that used by [1] to characterize liquid mirrors. The estimated stiffness values for case 1 and case 2 designs are  $3.31 \times 10^8$  N-m/rad and  $1.02 \times 10^8$  N-m/rad respectively.

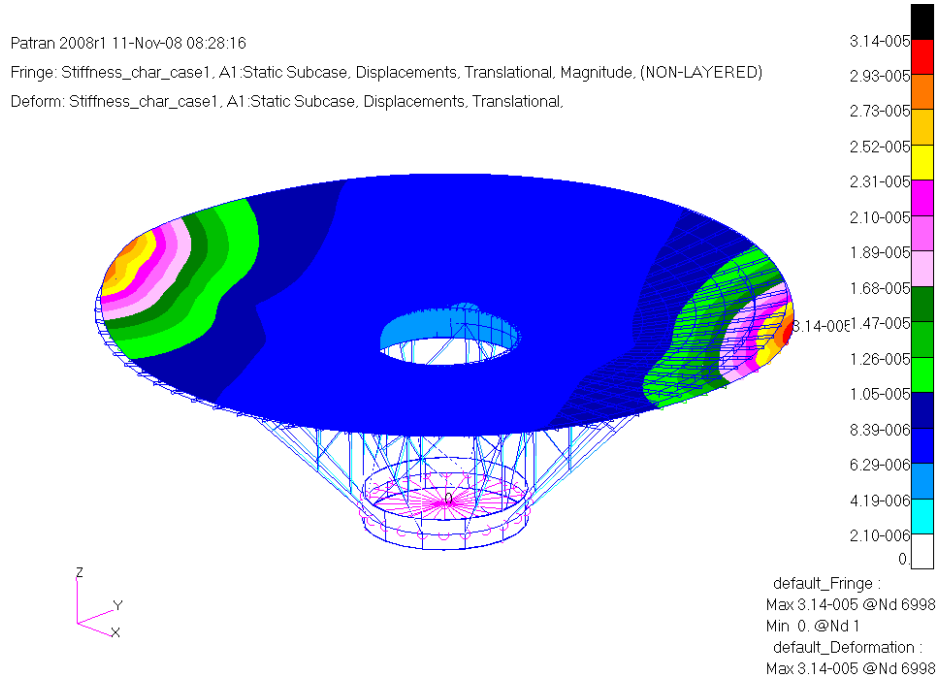


Figure 2-9: Stiffness characterization – case 1

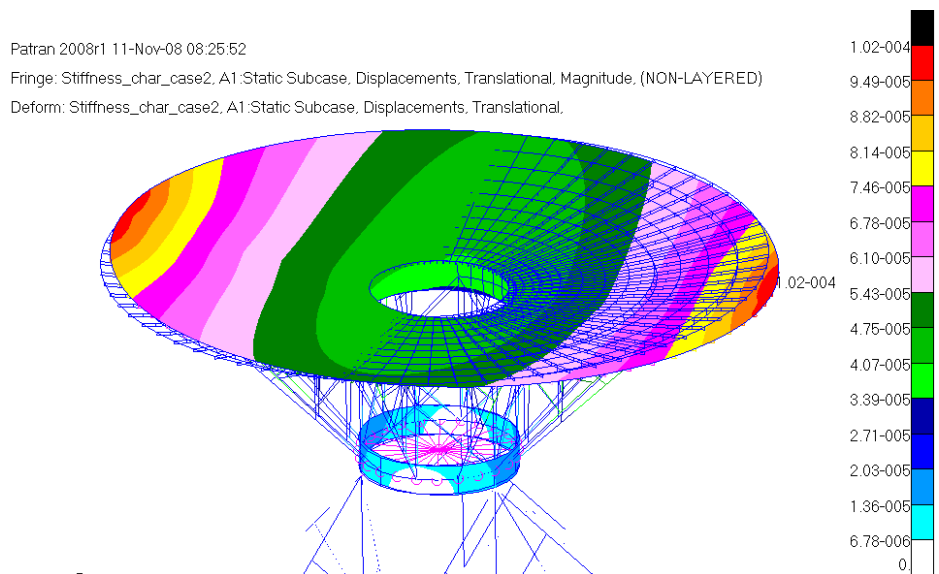


Figure 2-10: Stiffness characterization – case 2

## 2.10. Mirror tilting instabilities

Tilting instabilities, also referred to as whirling frequencies, are frequencies in which a perturbation in the tilt of the mirror can cause an unsteady response where the liquid will “slosh” from side-to-side causing runaway asymmetric loading. The criteria that [7] & [8] use to guarantee stability has the form:

$$\frac{4K_{\min}}{\pi\rho R^4} \geq 1 \quad (2)$$

where  $K$  is the effective structural stiffness,  $\rho$  is the liquid density, and  $R$  is the radius of the mirror. For a 20 m diameter mirror, the critical stiffness of the mirror structure is approximately  $2.0 \cdot 10^7$  N-m/rad. Since this is an order of magnitude below the anticipated stiffness of the structure, further mass reduction can be realized here through a more detailed study of mirror tilting instabilities.

## 2.11. Design Optimization

Looking at the major components of the LLMT, it can be clearly seen that the total stiffness of the telescope is a composite stiffness of the bearing and mirror structure. Since, the total stiffness of the LLMT follows an inverse sum rule,

$$\frac{1}{K_{Total}} = \frac{1}{K_{Structure}} + \frac{1}{K_{Bearing}} \quad (3)$$

by further increasing the stiffness of the bearing (and therefore the ratio of stiffness between the bearing and structure), will not yield effective results. This trend is demonstrated in Figure 2-11.

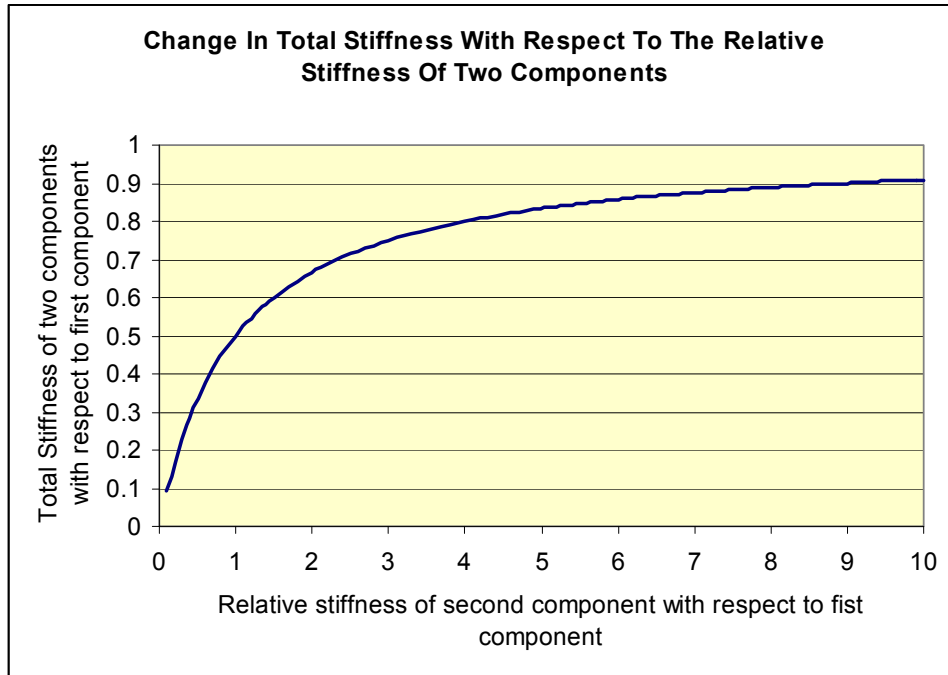


Figure 2-11: Total structural stiffness of a discrete two component system

As the estimated stiffness of the bearing is approximately five times greater than the stiffness of the mirror structure, mass savings can be achieved by reducing the mass of the bearing with minimal consequences in total stiffness. For example, reducing the bearing stiffness to three times the stiffness of the structure would only reduce the total stiffness by approximately 10%. Alternatively, great total stiffness gains can be achieved by increasing the structural stiffness, and therefore mass, slightly.

As performing a more detailed bearing design was considered out of the scope of this study, a brief optimization study of the mirror support structure was performed. Through modification to various section wall thicknesses, the change in structural mass and stiffness was examined. The effectiveness of the optimization was characterized through a stiffness-to-mass ratio focusing the optimization to achieve the highest possible structural stiffness per kg of mass.

It should be noted that buckling was not taken into consideration when performing the optimization, therefore growth in the total structural mass is anticipated to alleviate buckling concerns.

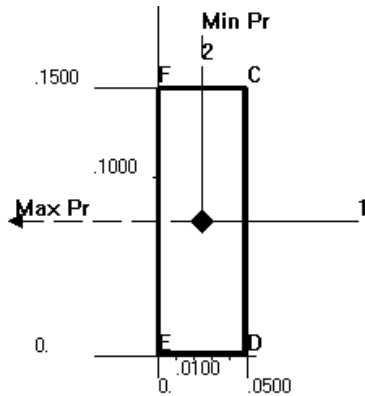


Figure 2-12: Rib support cross-section (dimensions in meters)

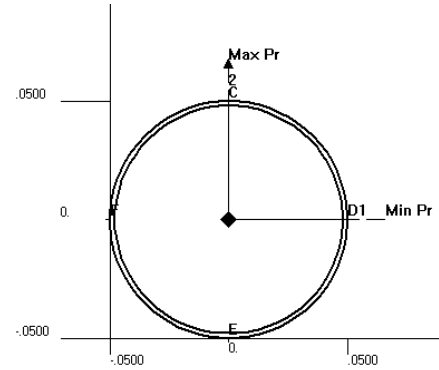


Figure 2-13: Truss beam cross-section (dimensions in meters)

The mirror panel support ribs are constructed of a single rectangular section shown in Figure 2-12, and are supported by the circular rib support beams pictured in Figure 2-13. The remaining truss structure is constructed of pin-jointed tubing of various sizes. Due to time limitations, the optimization was only performed on the structure above the bearing.

Table 3: LLMT design optimization results

	Stiffness/Mass (N-m / kg-rad)	Design change
A*	1.55	Truss wall: R=5cm, t=2mm Ribs t1/t2 wall thickness: 1mm/1mm
B*	1.36	Truss wall: R=5cm, t=1mm Ribs t1/t2 wall thickness: 1mm/1mm
C*	1.32	Truss wall: R=5cm, t=1mm Ribs t1/t2 wall thickness: 2mm/1mm
D*	1.57	Truss wall: R=7.5cm, t=2mm Ribs t1/t2 wall thickness: 1mm/1mm
E*	1.56	Truss wall: R=7.5cm, t=2mm; R=5cm, t=1mm Ribs t1/t2 wall thickness: 1mm/1mm
F*	1.57	Circular rib support beam: R=7.5cm t=3mm Truss wall: R=5cm, t=2mm; R=2.5cm, t=1mm
F	1.5	Circular rib support beam: R=7.5cm t=3mm Truss wall: R=5cm, t=2mm; R=2.5cm, t=1mm
G	0.37	Added case 2 support structure

\* bearing stiffness added analytically

Based on design optimization F, a mass breakdown of the mirror was performed and is displayed in the table below.

**Table 4: Estimated liquid mirror mass breakdown**

Component	Mass (kg)	kg/m <sup>2</sup>	Margin	Mass with margin (kg)	kg/m <sup>2</sup>
Liquid	400	1.1	30%	520	1.4
Mirror panel surface	940	2.6	30%	1222	3.4
Rib structure	785	2.2	30%	1021	2.8
Truss	298	0.8	30%	387	1.1
Load distributing ring and bearing structure	88	0.2	30%	114	0.3
Bearing	500	1.4	30%	650	1.8
<b>Case 1 total</b>	<b>3011</b>	<b>8.3</b>	30%	<b>3914</b>	<b>10.9</b>
Case 2 support structure	578	1.6	30%	751	2.1
<b>Case 2 total</b>	<b>3589</b>	<b>10.0</b>	30%	<b>4666</b>	<b>13.0</b>

It should be noted that even though case 2 looks less competitive from this initial primary mirror mass estimate, it is anticipated that there will be large mass savings in the fold-mirror support structure and other “down-light” components as they can be supported at ground level (unlike for case 1).

### 3. SUMMARY

The LLMT design is based on the need to optimize mass while maintaining high stiffness; allowing the structure to be compliant will reduce the overall structural mass substantially.

The current design of the LLMT includes a high bearing to mirror structure stiffness ratio and a factor for 10 for the critical stiffness required to avoid tilt instabilities. A detailed whirling analysis show that reductions in the bearing and mirror structural stiffness are possible, resulting in significant mass savings. During this process, the stiffness of the mirror panel surface (necessary to keep the mirror surface sag-free between rib elements) would have to be closely monitored as an optical grade surface (with liquid) is of paramount importance.

With a bearing diameter of ~5 m (the current aperture in the primary mirror), the bearing mass will be significant – even if a superconducting bearing is assumed. A mass estimate for a non-superconducting bearing (aluminum) may be as much as 800 kg.

The structural analysis shows that for a stiffness of  $\sim 3 \times 10^8$  N-m/radians, the structural mass would be on the order of 2000 kg – more than the ~1000 kg assumed in the NIAC report [5]. When considering the mass of the liquid and bearing, the LLMT primary mirror mass is estimated at 3011 kg, or 8.3 kg/m<sup>2</sup> for case 1 and 3589 kg, or 10.0 kg/m<sup>2</sup> for case 2. Once again, it should be noted that even though case 2 looks less competitive, it is anticipated that there will be large mass savings in the fold-mirror support structure and other “down-light” components as they can be supported at ground level.

Given these results it would seem that a mass to area of 10 kg/m<sup>2</sup> is achievable for a LLMT. This further implies that the component for a 20-m class LLMT could be delivered to the lunar surface with a future heavy lift vehicle such as the Ares-V. Thus a lunar based telescope with a >50% larger aperture than a space based telescope could be realized for the same launch costs. Of course the LLMT would require some lunar infrastructure for its assembly, but such infrastructure does allow for serviceability as well. Given the potential for this large aperture and the potential for good image quality at short wavelengths, liquid mirror telescopes remain a viable option for a future large aperture space telescope.

#### 4. ACKNOWLEDGEMENTS

The work described in this paper was undertaken as part of a Canadian Space Agency mission concept study, contract #9F028-070111/004/MTB, from December 2007 to December 2008. We gratefully acknowledge the support of the CSA, in particular our sponsors Jean Dupuis and James Doherty.

#### 5. REFERENCE DOCUMENTS

- [1] Postman, M., Brown, T., Koekemoer, A., Giavalisco, M., Unwin, S., Traub, W., Calzetti, D., Oegerle, W., Shull, M., Kilston, S., Stahl, H. P., "Science with an 8-meter to 16-meter Optical/UV Space Telescope," Proc. SPIE 7010, 701021 (2008).
- [2] Goldsmith, P., Bradford, M., Dragovan, M., Paine, C., Satter, C., Langer, B., Yorke, H., Haffenberger, K., Benford, D., Lester, D., "CALISTO: the Cryogenic Aperture Large Infrared Space Telescope Observatory," Proc. SPIE 7010, 701020 (2008).
- [3] Kendrick, S. E., "Monolithic versus segmented primary mirror concepts for space telescopes," Proc. SPIE, Vol. 7426, 74260O (2009).
- [4] Kendrick, S. E., Stahl, H. P., "Large aperture space telescope mirror fabrication trades," Proc. SPIE, Vol. 7010, 70102G (2008).
- [5] Angel, R., Worden, S. P., Borra, E. F., Eisenstein, D. J., Foing, B., Hickson, P., Josset, J-L., Ma, K. B., Seddiki, O., Sivanandam, S., Thibault, S., van Susante, P., "A Cryogenic Liquid-Mirror Telescope on the Moon to Study the Early Universe", *Astrophysical Journal* 680, 1582 (2008).
- [6] Hickson, P., Racine, R., "Image Quality of Liquid-Mirror Telescopes", *Pub. Astro. Soc. Pac.*, Vol. 119, 456–465 (2007).
- [7] Borra, E.F., "Liquid Mirrors: A Review," Centre d'Optique, Photonique et Lasers, Département de Physique, Université Laval, Canada
- [8] Content, R., "Design of 2-m to 6-m Liquid Mirror Containers," *Astronomical Instrumentation Group, Department of Physics, University of Durham, UK*